Target I.D. using natural resonances

A new concept for future radar systems

Michael A. Morgan

The need to quickly and accurately identify friends or foes at long distances in confrontational situations is essential to the maintenance of adequate defense. Also, essential is avoiding disastrous mistakes such as the downing of the Iranian Airbus in July 1988. Possible attack from high speed aircraft and missiles can require decisions regarding lethal engagement to be made within seconds of detecting an unknown "target."

This decision often relies upon the process of non-cooperative target recognition (NCTR). Current NCTR technology spans the gamut of information acquisition and processing, from simple visual observations to elaborate strategic systems which merge data from multiple sources including satellites and over-the-horizon radar.

In the realm of radar NCTR, there are two main categories: imaging and parameter identification. Imaging radars provide a visualization of the detected object using such techniques as focused spot scanning and inverse synthetic aperture. Parameter identification radars sense unique characteristics which are often not image related such as jet engine turbine rotation rates, hull vibration, or maneuvering patterns. Such radars typically utilize Doppler modulation of the received signal spectrum to sense differential motion of portions of the structure.

Use of electromagnetic natural resonance, as NCTR parameters is quite different from the conventional Doppler-based radar approach and is being investigated for use in future radar systems. Natural resonance frequencies contained in a target's radar signature are determined by its structure and can serve to identify the target. Further, the full set of natural resonances depend only upon the target's geometry and composition. They are independent of the target's position or orientation to the radar. This is an appealing property which lends simplicity to cataloging and identifying radar targets.

A mathematical description of electromagnetic natural resonances, termed the Singularity Expansion Method, was developed in 1971 by an electrical engineer at the Air Force Weapons Laboratory. In 1975, two EE professors from Ohio State University proposed that natural resonances could serve as an aspect-independent basis for radar NCTR. During the next several years, many researchers set out to estimate natural resonant modes in transient scattered fields by modeling the signature as a simple sum of complex exponentials (techniques that evolved from Prony (circa 1795)). This signal model was found to be incomplete in 1982 when attempts to estimate resonances using scattering measurements were made at the Naval Postgraduate School. New signal models were derived by this author in 1983 based upon the causal interactions which occur in transient electromagnetic scattering.

Physics of natural resonances

Electromagnetic natural resonances are determined by the target's structure in a manner analogous to that of the acoustical case. An important feature of natural resonances is the independence of their frequencies from the excitation that generates them. Consider, for example, the normal plucking of a guitar string, without force large enough to create nonlinear behavior. Once the string has been plucked, the resulting vibration, which produces the sound, will continue and will be a mixture of harmonically related natural resonance modes of the form

$$y(x,t) = \sum_{n=0}^{\infty} A_n(x) e^{\sigma_n t} \cos(\omega_n t + \theta_n(x)) \quad (1)$$

where $y(x,t)$ denotes the time-varying perpendicular displacement of the string from its normal position. Although the amplitude, $A_n(x)$, and phase, $\theta_n(x)$ of each mode in the string vibration will depend upon how and where the string was excited, the decay constant, σ_n ,and frequency, ω_n will be *independent* of both the position x and the form of the excitation applied to the string. Complex combinations of $s_n = \sigma_n + j\omega_n$ are termed the natural resonant frequencies and are determined only by the length, composition, and tension of the string.

If one were to digitize and process the acoustic signal provided by the string to deduce the values of s_n present, it would be easy to identify which string on the guitar had been excited, independent of where or how it had

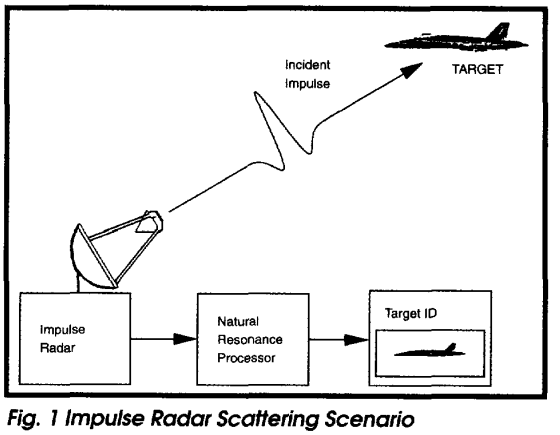

Fig. 1 Impulse Radar Scattering Scenario

0278-6648/93/$3.00 © 1993 IEEE

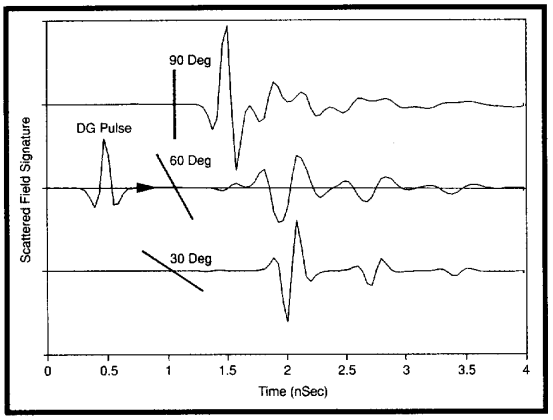

Fig. 2 Measured Scattering for a 10 cm Thin-Wire

been plucked. In a like manner, electromagnetic natural resonant frequencies do not depend upon the directions of arrival or reflection of the incident radar signal, nor upon the orientation of the object.

Consider a conducting radar target, such as an aircraft, being illuminated by an impulsive plane wave field having finite time duration, as depicted in Figure 1. The incident pulse induces currents as it travels at light velocity over the target's metal surface. These currents are influenced at each point on the target by two factors: 1) time behavior of the illuminating pulse at the surface point; and, 2) combined behavior of the current at all other surface points at earlier times. This influence is expressed by the time-domain magnetic field integral equation, which can be accurately approximated by

$$\bar{J}(p,t) = \bar{\bar{F}}(p,t) + \sum_{p'} \bar{\bar{K}}(p',p) \cdot \bar{J}\,[p', t - t_0(p',p)] \qquad (2)$$

where the vector surface current, $\bar{J}$, has been interpolated using values at selected surface points, having index p at time t, while $\bar{\bar{F}}(p,t)$ is proportional to the incident field at the pth point and is termed the "physical optics" current. The time delay, $t_0(p',p)$, is for straightline travel at light velocity between points p' and p, and the weighting kernel, $\bar{\bar{K}}(p',p)$, also depends upon this path length.

The summation in (2) provides the "feedback" current at each point due to the induced current at all other points. At sufficiently high frequencies, this feedback current becomes very small on the illuminated side of the target, resulting in $\bar{J} \rightarrow \bar{\bar{F}}$ while it tends to cancel the physical optics current on the shadow side, producing $\bar{J} \rightarrow \bar{0}$.

At somewhat lower frequencies, termed the resonance region, where major structural dimensions of the radar target are from a fraction to several wavelengths, the feedback current and the resultant natural resonance modes become quite significant.

Once the incident pulse has completed its illumination, so $\bar{\bar{F}} = \bar{0}$ in (1), the induced current will continue to circulate back upon itself (via the summation) in the form of decaying natural modes. This occurs as it radiates its energy outward into the scattered field. The scattered field is produced as a weighted integral of this induced current, taking on the following form at the location of the radar receiver

$$\bar{E}^s(t) = \bar{E}^s_{PO}(t) + \sum_{n=\infty}^{\infty} \bar{E}^s_n(t) e^{s_n t} \qquad (3)$$

Physical optics current in (2) produces $\bar{E}^s_{PO}$ while the summation of natural modes is due to the feedback process. Complex resonant frequencies, s_n depend only upon the physical structure of the radar target and are independent of the illuminating field. The exponentials in the summation of *(3)* could easily be combined as pairs of $\pm$ terms using Euler's identity, $\cos(u) = (e^{ju} + e^{-ju})/2$, to form a sum of damped cosines which is similar to that in (1).

Time-variation in each $\bar{E}^s_n(t)$ is due to the startup of the corresponding induced current mode as it reacts to the incident pulse moving across the radar target. Once the pulse completes its illumination of the target, induced current modes will have established their full spatial distribution. The modal amplitudes, $\bar{E}^s_n$ assume constant values after this time and the physical optic field vanishes.

This event separates the so-called "early-time" and "late-time" intervals whose transition depends upon the object geometry, the incident field behavior (e.g. angle of arrival and pulse width), and the observation point.

Sampled backscattering signatures measured at the Naval Postgraduate School are shown in Figure 2 for the case of a double-Gaussian (DG) pulse incident upon a 10 cm long thin wire, with diameter of 2.4 mm, for three different angular orientations from end-on. The incident electric field polarization is parallel to the wire in the case of the upper waveform (90 Deg). At the same time, the top of the wire is tilted increasingly forward towards the radar in the two lower waveforms, as illustrated.

The DG excitation pulse appearing in the figure is composed of two overlaid Gaussian waveforms, one having positive polarity with a 0.15 nSec 10% width and the other having negative polarity and a 10% width of 0.30 nSec. The relative amplitudes of the two Gaussians are set to provide zero area under the DG waveform (since d.c. cannot be radiated). This DG pulse provides an effective measurement bandwidth exceeding 1 to 13 GHz.

Initial early-time responses from the various orientations on the wire are made up of DG pulse driven currents and natural mode startups. The early-time interval for the thin-wire is the sum of the incident pulse width ($\approx$ 0.40 nSec) plus $2L \cos\theta_i/c$, where L is 10 cm, c is the velocity of light (30 cm/nSec), and θ_i is the incidence angle from end-on. In the upper waveform ($\theta_i = 90°$), the early-time is essentially the DG pulse width and the signature appears as a distorted replica of the DG pulse. The late-time response is composed of natural modes having the form of the sum in either (3) or (1).

For the canted incidence cases (θ_i = 30° and 60°) the early-time response is quite weak. In these cases, the driven current initially travels with the incident field while radiating strongly in the forward scattered direction and weakly in the backscattered direction. This traveling wave current then encounters the far end of the wire and is reflected by the open circuit at the same time as the leading edge of the incident pulse passes over the far end of the wire. The reflected traveling wave, which is due to the natural mode series, provides intense radiation in the backscattered direction and is the source of the delayed pulse

response (with inverted and distorted DG shape) for the canted cases. The following sequence of decaying pulses are due to periodic reflections of the natural mode traveling wave current from the far end of the wire as it continues to reflect back and forth from both ends of the wire.

A second set of measured target signatures is shown in Figure 3 for the case of a metal scale-model F-102A delta-wing fighter aircraft of length 21 cm and 12 cm wingspan. The same DG pulse illumination as shown in Figure 2 was used. The electric field polarization remained parallel to the wings as the aircraft model was rotated from nose-on aspect (labeled Nose) to nose-down, top illuminated aspect (Top) to tail-on aspect (Tail). The Nose signature displays an initial small response from the nose and leading edge wing followed later by a much larger response caused by traveling wave current reflection from the trailing edge of the delta-wing.

For Nose aspect, initial induced traveling wave currents on the sloped delta-wing and the fuselage radiate strongly in the forward direction. However, they contribute very little in the backscattered direction. This is similar in nature to the canted thin-wire cases, but with faster damping due to the larger radiating surface of the wing.

The Top aspect provides a highly coherent backscattered return from the fuselage and wing, followed by radiation from natural mode currents which continue to oscillate, much as for the 90° thin-wire case. The Tail aspect shows a strong return from the straight trailing wing edge, which is perpendicular to the fuselage (and parallel to the incident electric field), followed by only small natural mode returns.

Although the scattered waveforms for various aspects on a given target appear quite different, the complex natural resonant frequencies, which are embedded in the signatures, are the same and can be used, in principle, to identify the target.

Natural resonance estimation

Natural resonance NCTR approaches require identification of the target's complex resonances using the measured radar signature. This can occur either through comparison with a pre-established resonance data base or through processing of the measured signature using target-specific filters designed using known target resonances.

If sampled at discrete times $t = m\Delta t$ the scattered field in (2) can be described by

$$E^s[m] = \begin{cases} E_e^s[m] & \text{for } 0 \le m \le M \\ \sum_{n=-\infty}^{\infty} A_n (Z_n)^m & \text{for } m > M \end{cases} \quad (4)$$

where $\bar{E}_e^s$ [m] is the early-time scattered field which ceases for $m > M$. This term includes both physical optics and initializing resonance series contributions. The latetime summation of resonances is turned on at $m = M$. The z-plane poles in *(4)* contain the s-plane natural resonances of the radar target $Z_n = e^{s_n \Delta t}$.

The sampled signal in *(4)* solves an auto-regressive moving-average (ARMA) difference equation,

$$E^s[m] = \sum_{k=1}^{N} b_k E^s[n-k] + \sum_{i=0}^{L} a_i E^i[m-i] \quad \text{for } m \ge 0 \quad (5)$$

where $E^i[m]$ is the time-sampled incident field. The second sum represents the sampled physical optics scattered field in (3) while the recursive sum corresponds to the resonance series.

Once the incident pulse has completed its illumination of the target, the radiated field will solve an auto-regressive (AR) form of (5) sans the sum on $E^i[m—i]$. This late-time AR signal model is the basis for Prony's two-step method. First, the $E^s[m]$ values are used to estimate the b_k coefficients. The b_k values are then used to form an N-th order polynomial in z whose complex roots are the poles being sought. This simple procedure is, however, highly sensitive to noise or errors in the measured signal.

Two reasons for this sensitivity are that the noise does not satisfy the system model in (5) and the system order, N, is generally not known. When the estimated order is greater than the actual order, poles due to noise are generated. Prony's method offers no technique for distinguishing signal poles from the extra poles caused by overestimation of the system's order. If the estimated system order is less than the actual order, true poles are lost and the remaining poles are perturbed from their correct positions.

Various approaches to this difficult estimation problem have been developed in the last decade. One such method employs a reversed-time ARMA model for the input and output of the system to yield both the poles and zeros of the target. The model order is overestimated to allow data fitting to the noise and an overdetermined system is formed. A pseudoinverse is found based on singular value decomposition (SVD). When reversed-time processing is employed, the SVD algorithm allows discrimination of target and noise poles by forcing them into distinct regions of the z-plane bounded by the unit circle.

Examples of estimated z-plane poles are shown in Figure 4 for backscattering from the 10 cm thin-wire considered in Figure 2. Poles for four different θ^i incident angles are overlaid on the plot. Estimated target poles are inside of the right-half unit circle, which corresponds to frequencies from d.c. to 12.7 GHz (corresponding closely to the upper frequency of the illuminating DG pulse). Numerous extra poles which model the noise are also observed, but outside of the unit circle (courtesy of the SVD algorithm), and mostly in the left-half plane, where the unit circle represents frequencies of 12.7 to 25.4 GHz.

Clustering of the target poles is due to their aspect independence. Tightness

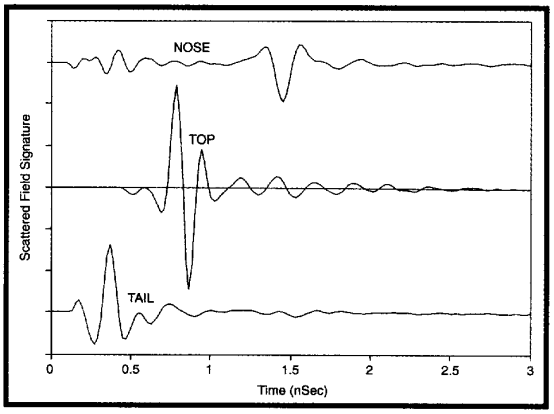

Fig. 3 Measured Scattering for a Scale Model F-102A Aircraft

of these clusters is an indication of how well the algorithm is estimating the actual pole locations. It should be noted that only half of the target poles are found for broadside (90°) illumination. In this special case, resonances having odd symmetry are not excited since there is even symmetry in both the incident field and the structure.

Estimated z-plane poles for the F-102A scale-model aircraft are overlaid in Figure 5 for the three radically different aspects previously considered. Clearly defined target pole clusters are apparent within the unit circle on the right-half while noise poles appear outside the unit circle at frequencies beyond the excitation bandwidth in the left-half z-plane.

Real world implementation

Natural resonance NCTR is most effective using frequencies within the resonant region of the target. A somewhat arbitrary criterion is that major target dimensions are in the range of, say, 0.4 to 4 wavelengths. For the case of a tactical fighter aircraft, with typical length or wingspan of 25 m, this criterion gives a resonance region of 4.8 to 48 MHz. Such a 10:1 bandwidth is only hypothetical and may be much less in practical NCTR. Natural resonance NCTR will, in any case, require an ultra-wideband radar system which excites full structure resonances on the target, typically operating in the HF to VHF frequency bands for air targets.

Although a small impulse radar provides outstanding measurement quality in the enclosed laboratory at the Naval Postgraduate School, such an approach on a full-scale basis is wrought with the side effects of indiscriminant electromagnetic interference to communications, telemetry, signal intercept, and other radars. Proponents of impulse radars argue that energy transmitted to any narrow bandwidth system will be small and cyclic, at the impulse rate used. This periodic interference may have serious effects in raising the bit-error rates of some digital systems to unacceptable levels.

An adaptive stepped-frequency system is the viable alternative to impulse radar in real-world applications requiring ultra-wide bandwidth. Spectrum control would allow the radar to step over any designated frequency ranges, on the fly, thus avoiding interference. An ultra-wideband impulse response could be obtained, if desired, using high-speed signal processing and inverse transforms.

Finally, natural resonance based NCTR, if implemented, will most likely be used to augment more conventional long-range search and tracking radars. The resonance information provided can be combined with other deduced features, such as high-resolution imaging and trajectory dynamics, to assess the target's identity.

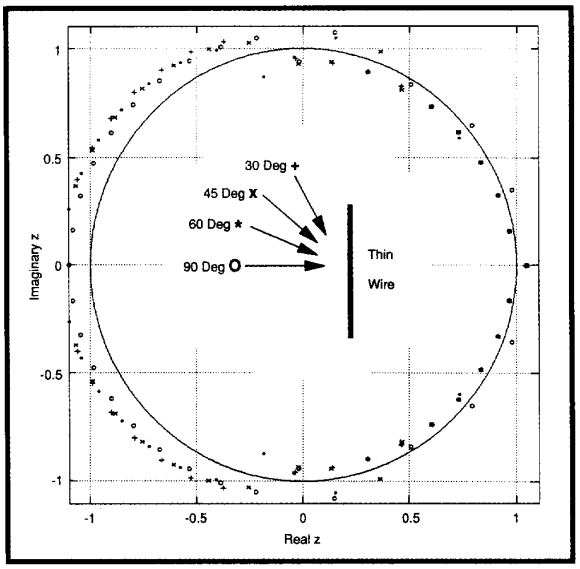

Fig. 4 Estimated Z-Plane Poles for a 10 cm Thin-Wire at Four Aspects

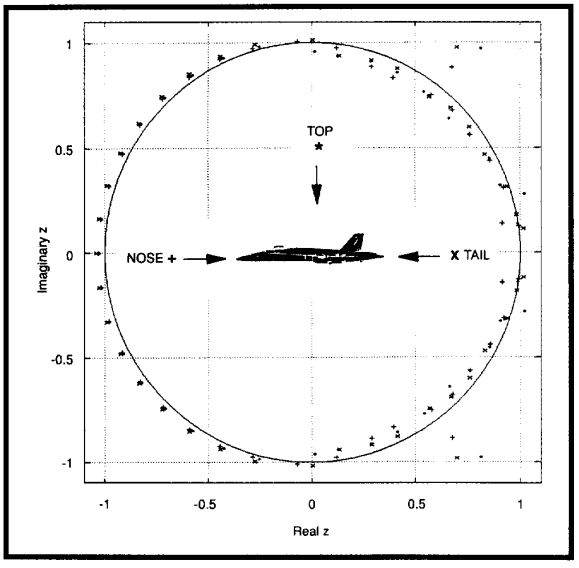

Fig. 5 Estimated Z-Plane Poles for a Scale Model F-102A Aircraft at Three Aspects

Read more about it

- C.E. Baum, E.J. Rothwell, K.-M. Chen, and D.P. Nyquist, "The singularity expansion method and its application to target identification," *Proceedings of the IEEE*, vol. 79, pp. 1481-1492, October 1991.
- M.A. Morgan and N.J. Walsh, "Ultra-wideband transient electromagnetic scattering laboratory," *IEEE Trans. on Antennas Propagat.*, vol. AP-39, pp. 1230-1234, August 1991
- J.A. Cadzow and O.M. Solomon, Jr., "Algebraic approach to system identification," *IEEE Trans. Acoustics, Speech and Sig. Proc.*, vol. ASSP-34, pp. 462-469, June 1986.
- M.A. Morgan and P.D. Larison, "Natural resonance extraction from ultra-wideband scattering signatures," in *Ultra-Wideband Radar: Proceedings of the First Los Alamos Symposium*, B.W. Noel, Ed., Boca Raton: CRC Press, 1992.

About the author

Michael A. Morgan has been a faculty member at the Naval Postgraduate School since 1979 and has served as Chairman of the Electrical and Computer Engineering Department since 1990. While on leave of absence in 1985-86, he managed the basic research program in electromagnetics at the Office of Naval Research. His research interests include computational electromagnetics and target identification.